American Institute of
Aeronautics and Astronautics

# INCORPORATING SECULAR DRIFTS INTO THE ORBIT ELEMENT DIFFERENCE DESCRIPTION OF RELATIVE ORBITS

Hanspeter Schaub

# 13th AAS/AIAA Space Flight Mechanics Meeting

# INCORPORATING SECULAR DRIFTS INTO THE ORBIT ELEMENT DIFFERENCE DESCRIPTION OF RELATIVE ORBITS

Hanspeter Schaub [*]

To describe the linearized relative motion between two spacecraft in near circular orbits, the classical Hill's or Clohessy-Wiltshire equations can be analytically solved with time being the independent variable and the relative position vector being expressed in terms of the Cartesian components of the rotating Hill coordinate frame. However, as the eccentric chief orbits are considered, finding an analytical solution to the linearized relative motion in terms of these Cartesian coordinates becomes very challenging. In recent developments an equivalent set of relative orbit equations has been presented where the linearized relative orbit geometry is described through orbit element differences and the true anomaly angle is used as the independent variable. Their algebraic structure is very similar to the solution of the circular chief orbit Clohessy-Wiltshire equations. However, this linearized relative motion description can also scale easily to the eccentric chief orbit case. If the orbit element differences are not constant, but vary due to perturbations such as the $J_2$ gravitational perturbation, or the mean anomaly difference varies due to unequal orbit energy states, then the orbit element difference differential equations would need to be integrated with respect to time while simultaneously solving Kepler's equation to relate time and true anomaly. This paper presents a method which can avoid this numerical integration by finding, where possible, analytical approximations to the orbit element difference time histories in terms of the true anomaly angle. With these equations it is possible to describe the long term linearized relative Cartesian motion of spacecraft formation, including secular drift behavior, until the inter-satellite separation is no longer small compared to the chief orbit radius and the linearization assumptions fail.

## INTRODUCTION

The study of spacecraft formation flying dynamics and control has enjoyed a remarkable resurgence during the last few years. The driving force behind this interest are envisioned space missions where the science requirements demand large distances between various sensors nodes. These requested separations can vary from as small as a few dozen meters to as large as multiple kilometers. Further complicating these missions is the requirement that the *relative* sensor positions must be maintained to a high degree of accuracy. For example, the Techsat 21 program is looking at using a multitude of spacecraft to form sparse aperture radar system with a dish diameter of up to 1 kilometer. Building a structure that is of the order of kilometers in size is an extremely challenging and expensive proposition. Having free-flying satellites at the required sensor nodal points appears to be a more promising solution. However, to avoid excessive fuel consumption to maintain specified relative orbits,

[*]Aerospace Research Engineer, ORION International Technologies, Albuquerque, NM 87106.

it is crucial that the actual relative orbits be as close as possible to naturally occurring bounded relative motion solutions.

A large class of spacecraft formation flying missions is to have a near-circular chief satellite orbit. In this simplified case the classical Hill's or Clohessy-Wiltshire (CW) equations have been extensively used to determine suitable relative orbits. For this circular chief orbit case, the CW equations can be solved analytically using time as the independent variable. The Cartesian coordinates $(x, y, z)$, expressed in the rotating Hill frame, are provided as a function of various trigonometric terms as well as a secular term. Having an analytical solution to the relative motion is very useful for the mission designers trying to determine what relative orbit solutions meet the science requirements, as well as the guidance and control design engineers trying to find feedback control laws to establish and maintain a specific relative orbit.[1]

However, the classical solution to the CW equations is limited to the circular chief orbit case. To find the relative motion with eccentric chief orbits, typically numerical integration schemes are employed. Solving the relative differential equations of motion for the general elliptic chief orbit case is a very challenging task that has been tackled in various papers. Melton develops in Reference 2 a state transition matrix that can be used to predict the relative motion for chief orbits with small eccentricities by using a series expansion in terms of time. Tschauner and Hempel have solved the relative equations of motion directly for the general case of having an elliptic chief orbit.[3] Later work by both Lawden and Carter further refined this relative motion solution to avoid singularities with circular chief orbits.[4] However, their solution is not explicit and requires the computation of an integral. Kechichian develops in Reference 5 the analytical solution to the relative orbit motion under the influence of both the $J_2$ and $J_3$ zonal harmonics assuming that the eccentricity is a very small parameter. Unfortunately these methods yield relatively complex solutions and the six Cartesian relative motion initial conditions do not easily reveal the geometry of the resulting relative orbit. Broucke has presented in Reference 6 an analytical solution to the linearized relative equations of motion for eccentric chief orbits. His solution uses both time and true anomaly and finds the current Cartesian coordinates of a deputy satellite given the initial Cartesian coordinates.

Often the six initial Cartesian position and velocity coordinates in the rotating Hill frame are used as the relative motion invariants. An alternate set of six invariant parameters are the orbit element differences relative to the chief orbit.[7–11] Linearizing the nonlinear relative motion in terms of small differences in orbit elements will yield more accurate results than when rectilinear, or even curvilinear, Cartesian coordinates are used.[12] In References 7 and 8 the anomaly angle difference is prescribed in terms of the mean anomalies, not the true or eccentric anomaly, since the mean anomaly difference between two satellites remains constant (assuming equal orbit energy states) even for eccentric chief orbits. Prescribing the relative orbit geometry through sets of orbit element differences has the major advantage that these relative orbit coordinates are constants of the non-perturbed orbit motion if the orbit energies are constant. Once perturbations are introduced, these orbit element differences will typically vary only very slowly. In contrast, the typical $(x, y, z)$ Hill coordinates of the relative motion are fast variables which change rapidly during the entire orbit. Further, well established analytical theories are available that describe how these orbit elements will change due to, for example, the $J_2$ gravitational perturbation or atmospheric drag.

While the CW frame relative orbit description is only a linearized approximation to the true relative motion, the orbit element difference description itself is valid for relative orbits of arbitrary size. Defining a relative orbit to only have mean anomaly difference $\delta M$ will result in a classical leader-follower relative orbit, no matter what the relative orbit dimension is. Assuming Keplerian orbit motion, the classical orbit equation $r = p/(1 + e \cos f)$ provides the radial satellite motion within its constant orbit plane. Making use of the orbit orientation angles, it is always possible to analytically compute the inertial orbit motion $(X, Y, Z)$ of each satellite. By differencing these inertial position vectors and expressing the result terms of the Cartesian Hill frame coordinates, it is possible to write the analytic solution of the unperturbed, nonlinear relative motion problem in terms of the Cartesian Hill frame components by using the orbit elements to define the inertial orbit motion. However, this general nonlinear analytic solution to the relative motion problem is algebraically complex and provides little insight into the nature and geometry of the relative orbits given initial orbit element differences.

In References 13 and 14 a first order mapping between orbit element differences and the corresponding Hill frame Cartesian coordinates is presented. This allows the linearized relative motion to be written as an explicit function of the true anomaly and the orbit element differences. By sweeping the true anomaly through a range of angles, the corresponding relative orbit motion is directly determined without having to solve any differential equations. While the orbit element difference description of a relative orbit does not make any assumptions on the size of the relative orbit, this first order mapping to and from Cartesian Hill frame coordinates does assume that the relative orbit size is small compared to the chief inertial orbit radius. Whereas the analytical solution to the circular chief CW equations provides $(x(t), y(t), z(t))$ as a function of the initial position and velocity coordinates, the orbit element description provides an equivalent set of relative orbit coordinates $(x(f), y(f), z(f))$ with true anomaly as the independent variable. In essence, the elegant analytical solution of the linear CW equations, which is limited to the circular chief orbit special case, is extended for elliptic orbits. The general solution for chief orbits with arbitrary eccentricities was shown in Reference 14. If the orbit element differences vary with time, then the solution in Reference 14 requires the orbit element and orbit element difference differential equations to be solved.

The research presented in this paper extends the work presented in Reference 14 by incorporating analytical results to accommodate relative orbits with certain types of secular drifts. These drifts could be due to having different orbit periods (orbit energy states), or due to perturbations such as the $J_2$ gravitational attraction or atmospheric drag. Whenever possible, approximate analytical solutions are presented in terms of the true anomaly angle which avoid the need to numerically integrate the orbit element drifts. With these analytical equations the effect of the particular perturbations can be seen in the linearized relative motion description. The approximations are valid as long as the linearizing assumption that the relative orbit size is small compared to the inertial chief orbit radius is satisfied. Whereas the analytical solution to the linear CW equations includes the drift due to unequal orbit periods, the linearized relative orbit description using orbit element differences is also able to incorporate the drift due the $J_2$ gravitational perturbation in an analytical manner. While valid for orbits of any eccentricity, the structure of the algebraic expressions of the linearized relative orbit motion reduces to an equivalent algebraic structure of the classical

CW analytical solution if the chief orbit becomes circular.

## RELATIVE ORBIT DESCRIPTION REVIEW

To express how the relative orbit geometry of the deputy satellite is seen by the chief (primary point of reference), the Hill coordinate frame $\mathcal{O}$ is introduced.[15] Its origin is at the osculating chief satellite position and its orientation is given by the vector triad $\{\hat{\boldsymbol{o}}_r, \hat{\boldsymbol{o}}_\theta, \hat{\boldsymbol{o}}_h\}$ shown in Figures 1. The unit vector $\hat{\boldsymbol{o}}_r$ is in the orbit radius direction, while $\hat{\boldsymbol{o}}_h$ is parallel to the orbit momentum vector in the orbit normal direction. The unit vector $\hat{\boldsymbol{o}}_\theta$ then completes the right-handed coordinate system. Let $\boldsymbol{r}$ be the chief orbit radius and $\boldsymbol{h}$ be the chief angular momentum vector. Unless noted otherwise, any non-differenced states or orbit elements are assumed to be those of the chief. Differenced states are assumed to be differences between the deputy and chief satellite. Mathematically, these $\mathcal{O}$ frame orientation vectors are expressed as

$$\hat{\boldsymbol{o}}_r = \frac{\boldsymbol{r}}{r} \tag{1a}$$

$$\hat{\boldsymbol{o}}_\theta = \hat{\boldsymbol{o}}_h \times \hat{\boldsymbol{o}}_r \tag{1b}$$

$$\hat{\boldsymbol{o}}_h = \frac{\boldsymbol{h}}{h} \tag{1c}$$

with $\boldsymbol{h} = \boldsymbol{r} \times \dot{\boldsymbol{r}}$. Note that if the inertial chief orbit is circular, then $\hat{\boldsymbol{o}}_\theta$ is parallel to the satellite velocity vector.
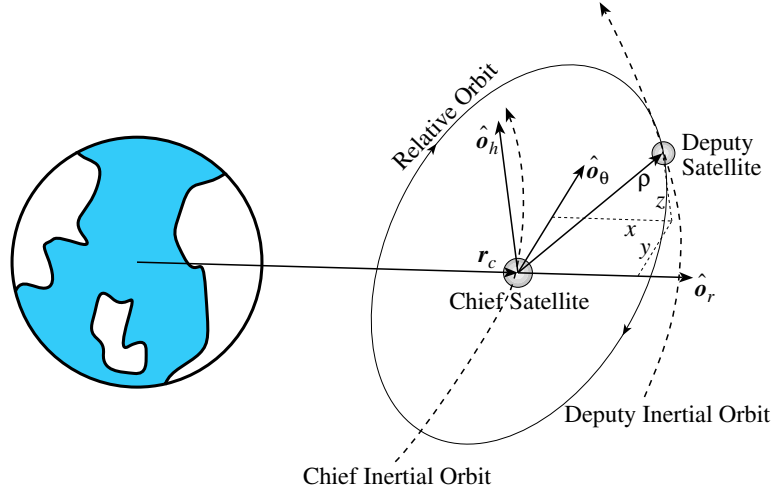


**Figure 1: Illustration of the Cartesian Hill Frame Coordinates of a Relative Orbit**

The relative orbit position vector $\boldsymbol{\rho}$ of a deputy satellite relative to the chief is expressed in Cartesian $\mathcal{O}$ frame components as

$$\boldsymbol{\rho} = (x, y, z)^T \tag{2}$$

If the chief orbit is circular or near-circular, then the linearized relative equations of motion are given through the famous Clohessy-Wiltshire or CW equations.[16] These are sometimes

also referred to as Hill's equations.[15]

$$\ddot{x} - 2n\dot{y} - 3n^2x = 0 \tag{3a}$$

$$\ddot{y} + 2n\dot{x} = 0 \tag{3b}$$

$$\ddot{z} + n^2z = 0 \tag{3c}$$

Further, these differential equations are only valid if the relative orbit radius is small compared to the planet-centric orbit radius. The differential CW equations can now be solved for an analytical solution of the linearized relative orbit motion.

$$x(t) = A_0 \cos(nt + \alpha) \tag{4a}$$

$$y(t) = -2A_0 \sin(nt + \alpha) + (\dot{y}_0 + 2nx_0)t + y_{off} \tag{4b}$$

$$z(t) = B_0 \cos(nt + \beta) \tag{4c}$$

The integration constants $A_0$, $B_0$, $\alpha$, $\beta$ and $y_{off}$ are determined through the relative orbit initial conditions and $n$ is the mean orbital frequency $n = \sqrt{\mu/a^3}$. If the initial conditions satisfy $\dot{y}_0 + 2nx_0 = 0$ (i.e. the orbit periods are equal), then the linearized relative orbit will have a bounded motion determined through sinusoidal terms and a potential static offset in the along-track direction. Please note that while the CW equations in Eq. (3) are shown for a set of Cartesian coordinates, the same set of differential equations are also valid if these $(x, y, z)$ coordinates are interpreted to be curvilinear coordinates with $x = \delta r$ being a difference of orbit radii and $y = r\delta\theta$ being the curved along-track motion. The angle $\theta = \omega + f$ is the true latitude angle. Making this curvilinear coordinates assumption greatly increases the predicted relative orbit accuracy of the CW equations.

Let us define the orbit element difference vector $\delta\boldsymbol{e}$ to consist of

$$\delta\boldsymbol{e} = (\delta a, \delta M, \delta i, \delta\omega, \delta e, \delta\Omega)^T \tag{5}$$

Note that all these orbit element differences, except for $\delta M$, are always constants of the Keplerian two-body motion. If the orbit periods are equal (i.e. semi-major axis are equal), then $\delta M$ is also constant, even for the eccentric chief orbit case. By dividing the dimensional $(x, y, z)$ relative orbit coordinates by the time varying chief orbit radius $r$, we obtain the non-dimensional relative orbit coordinates $(u, v, w)$. Reference 14 introduces the following analytical approximate solution of the linearized relative orbit motion in terms of the orbit element differences $\delta\boldsymbol{e}$:

$$u(f) = \frac{\delta a}{a} - \frac{e\delta e}{2\eta^2} \qquad\qquad + \frac{\delta_u}{\eta^2}\left(\cos(f - f_u) + \frac{e}{2}\cos(2f - f_u)\right) \tag{6a}$$

$$v(f) = \left(\left(1 + \frac{e^2}{2}\right)\frac{\delta M}{\eta^3} + \delta\omega + \cos i\,\delta\Omega\right) \quad - \frac{\delta_u}{\eta^2}\left(2\sin(f - f_u) + \frac{e}{2}\sin(2f - f_u)\right) \tag{6b}$$

$$w(f) = \qquad\qquad\qquad\qquad\qquad \delta_w \cos(\theta - \theta_w) \tag{6c}$$

The parameter $\eta = \sqrt{1 - e^2}$ is another convenient eccentricity measure and the small states $\delta_u$ and $\delta_w$ are given through

$$\delta_u = \sqrt{\frac{e^2\delta M^2}{\eta^2} + \delta e^2} \tag{7a}$$

$$\delta_w = \sqrt{\delta i^2 + \sin^2 i \delta \Omega^2} \tag{7b}$$

while the phase angles $f_u$ and $\theta_w$ are expressed as

$$f_u = \tan^{-1}\left(\frac{e \delta M}{-\eta \delta e}\right) \tag{8a}$$

$$\theta_w = \tan^{-1}\left(\frac{\delta i}{-\sin i \ \delta \Omega}\right) \tag{8b}$$

Note that Eq. (6) has a very algebraic similar structure to the CW solution in Eq. (4) in that the motion is expressed through trigonometric terms and static offsets. However, the solution in Eq. (6) is not only valid for circular chief orbits, but for orbits of any eccentricity. Reference 14 also presents simplified versions of this relative motion solution. In one case the chief orbit is assumed to be near-circular and only terms linear in the eccentricity $e$ are retained. In the other case the chief orbit is assumed to be circular and an equivalent solution to the CW equations in Eq. (4) is obtained by dropping all terms containing the eccentricity $e$. This general linearized relative motion solution is valid both if $\delta e$ is constant or time time varying. In the later case, as with *all* linearized relative motion solutions, the accuracy of the Cartesian relative motion predictions will break down if the linearizing assumption is no longer valid (i.e. the relative orbit radius is no longer small compared to the inertial orbit radius). If $\delta \dot{e} = 0$, then Eq. (6) provides an analytical solution of the linearized relative motion for general chief orbit eccentricities. If $\delta \dot{e} \neq 0$, then this solution requires the differential equations $\delta \dot{e}$ and $\dot{e}$ to be solved, along with Kepler's equation relating true anomaly and time, to determine the linearized relative motion in the Cartesian Hill frame coordinates.

## INCORPORATING SECULAR DRIFT

When designing the relative orbits, typically satellite orbits are chosen such that the relative orbit motion is bounded. However, depending on the mission requirements it can occur that relative orbits are chosen which contain a slow secular drift. For example, the $J_2$-invariant relative orbits presented in Reference 7 enforce that the mean ascending node drift $\delta \dot{\Omega}$ and the mean latitude drift $\delta \dot{\theta}_m = \delta \dot{\omega} + \delta \dot{M}$ are equal among satellites under the influence of the $J_2$ gravitational perturbation. However, for near circular or polar chief orbits it might be impossible to enforce both constraints, since they would dictate relative orbits with impractically large relative orbits. In such cases a certain amount of relative orbit drift is expected and will need to be compensated for with periodic relative orbit corrections. Another example would be the influence of differential drag. If the satellite are of equal type and build, then the $J_2$ perturbation will have a more dominant effect on the relative orbit. However, if some satellites have consumed more fuel than others, then they will no longer be of equal type and build and the differential drag will cause a more noticeable secular drift of the relative formation.

If the relative orbits are not bounded, then the orbit element differences will not remain constant. Note that as long as the relative orbit size has not grown too large, the equations of motion in Eq. (6) are still valid. However, due to the drifts the orbit element differences $\delta e$ must now be treated as time varying quantities. Assume that a differential equation

$\delta \dot{\boldsymbol{e}}$ is given which describes how the orbit elements will drift. This drift could be due to having orbits of unequal orbit periods, or because non-Keplerian influences such as the $J_2$ gravitational perturbation or atmospheric drag are present. One brute force method to accommodate $\delta \dot{\boldsymbol{e}}$ is to simplify integrate these equations with respect to time. However, Eq. (6) uses the true anomaly as the independent variable. Thus, at each time step Kepler's equation would have to be solved to map the true anomaly $f$ into a corresponding time state $t$ and then evaluate the required $\delta \boldsymbol{e}\,(t(f))$. This section investigates more elegant solutions. Where possible, approximate analytical solutions are provided expressing the orbit element drifts directly in terms of the true anomaly. This avoids the need to perform any numerical integrations to study the approximate long-term behavior of relative orbits.

**Drift Due to Unequal Orbit Energies**

First, the relative orbit drift due to the deputy and chief satellite orbits having unequal energy levels is investigated. Standard Keplerian orbit motions are assumed. As is well-known from celestial mechanics, the orbit period is determined solely from the semi-major axis $a$. Ignoring other perturbations, if two orbits have unequal semi-major axes, then we expect the two anomaly angles to drift apart. Thus, having a non-zero $\delta a$ in Eq. (6) will result in the mean anomaly difference $\delta M$ having a secular drift. The chief mean anomaly $M$ is given by

$$M(t) = nt + M_0 = \sqrt{\frac{\mu}{a^3}}t + M_0 \tag{9}$$

where $M_0 = M(t_0)$. The mean anomaly rate is expressed as

$$\dot{M} = \frac{\mathrm{d}M}{\mathrm{d}t} = \sqrt{\frac{\mu}{a^3}} \tag{10}$$

Taking the first variation of Eq. (10), we find that small differences in mean anomaly rates $\delta\dot{M}$ are related to small differences in the semi-major axis $\delta a$ through

$$\delta\dot{M} = \frac{\mathrm{d}(\delta M)}{\mathrm{d}t} = -\frac{3}{2}\sqrt{\frac{\mu}{a^5}}\delta a = -\frac{3}{2}n\frac{\delta a}{a} \tag{11}$$

By defining these differences to be differences between deputy and chief satellite orbit elements, Eq. (11) provides an approximation to how the mean anomaly difference will vary due to $\delta a$. Note that the true nonlinear drift in mean anomalies is given by

$$\delta\dot{M} = \dot{M}_d - \dot{M} = \sqrt{\frac{\mu}{(a + \delta a)^3}} - \sqrt{\frac{\mu}{a^3}} \tag{12}$$

where $a_d = a + \delta a$. We could easily integrate Eq. (11) with respect to time to estimate the mean anomaly difference at a particular time step $t$. However, we would still have to solve Kepler's equation to relate a time $t$ to the corresponding true anomaly angle $f$ to make use of the relative orbit equations in Eq. (6). These are extra steps in evaluating the linearized relative orbit that are preferably avoided. Instead, the following steps will lead to an analytical solution of the linearized drift equation $\delta\dot{M}$. First the differential equation in

Eq. (11), which is expressed with respect to time, is rewritten to be expressed with respect to the true anomaly $f$. To accomplish this, we make use of the identity

$$\frac{\mathrm{d}t}{\mathrm{d}f} = \frac{r^2}{h} = \frac{\eta^3}{n(1+e\cos f)^2} \tag{13}$$

where $\eta = \sqrt{1-e^2}$. Multiplying both sides of Eq. (11) by $\mathrm{d}t/\mathrm{d}f$, we find

$$\delta M' = \frac{\mathrm{d}}{\mathrm{d}f}(\delta M) = -\frac{3}{2}\frac{\eta^3}{(1+e\cos f)^2}\frac{\delta a}{a} \tag{14}$$

The differential equation in Eq. (14) could be numerically integrated with respect to the true anomaly $f$ to find the required $\delta M(f)$ without having to solve Kepler's equation at each integration step. However, this differential equation can be solved analytically as well. Note that

$$\int_{f_0}^{f} \frac{\eta^3}{(1+e\cos f)^2} = \left. \left( E(f) - \frac{e\,\eta\sin f}{(1+e\cos f)} \right) \right|_{f_0}^{f} \tag{15}$$

Applying this integral solution to Eq. (14) yields:

$$\delta M(f) = \delta M_0 - \frac{3}{2}\left. \left( E(f) - \frac{e\,\eta\sin f}{(1+e\cos f)} \right) \right|_{f_0}^{f}\frac{\delta a}{a} \tag{16}$$

The variable $E$ is the eccentric anomaly and is related to the true anomaly $f$ through the transformation

$$E(f) = 2\arctan\left( \frac{\sqrt{1-e}\sin(f/2)}{\sqrt{1+e}\cos(f/2)} \right) \tag{17}$$

When numerically evaluating $E(f)$, note that the `atan2(x,y)` function should be used to avoid arctan() singularities and obtain angles in the proper quadrant. Thus, Eq. (16) provides a direct analytical approximation of the mean anomaly drift due to $\delta a$ in terms of the true anomaly $f$. Further, not that this $\delta M(f)$ approximation is valid for chief orbits of any eccentricity, as long as the relative orbit size has not grown large compared to the chief inertial orbit radius. The term $E(f)$ provides the expected secular term in $\delta M(f)$ due to the semi-major axis difference $\delta a$ and will grow unbounded with time. Further, combined with the general solution in Eq. (6), the $\delta M(f)$ solution in Eq. (16) provides a complete analytical solution of the linearized relative orbit motion for any Keplerian motion.

A common mission scenario is that the chief orbit only has a weakly eccentric orbit. The general expression in Eq. (16) can then be refined by neglecting higher order terms of the eccentricity $e$ and only retaining terms which are linear in $e$. Since we are already dropping higher order terms in $\rho/r$ to obtain the relative motion equations in Eq. (6), a weakly eccentric orbit is understood to be one where $e^n$ (with $n > 1$) is smaller than $\rho/r$ and $e$ is larger than $\rho/r$. For this case, the approximation of the mean anomaly drifts $\delta M(f)$ are expressed as

$$\delta M(f) = \delta M(f_0) - \frac{3}{2}\left. (f - 2e\sin f)\right|_{f_0}^{f}\frac{\delta a}{a} \tag{18}$$

8

If the chief orbit is essentially circular, then $e$ is virtually zero and much smaller than the relative orbit radius to inertial orbit radius ratio $\rho/r$. In this case, the approximation of the mean anomaly drifts $\delta M(f)$ is reduced to

$$\delta M(f) = \delta M(f_0) - \frac{3}{2}(f - f_0)\frac{\delta a}{a} \tag{19}$$

Note that either of these three $\delta M(f)$ equations could be used with the corresponding relative motion equations in Reference 14 for the strongly eccentric, weakly eccentric or non-eccentric chief orbit cases.

**Drift Due to the $J_2$ Gravitational Perturbation**

For low Earth orbits (LEO), the $J_2$ gravitational perturbation is the dominant perturbation for a formation with spacecraft of equal type and built. While the atmospheric drag will cause all satellite orbits to continuously loose energy, the deceleration is nearly identical among these spacecraft. Thus, the atmospheric drag effect on the relative formation geometry is minimal over a time span of several orbits. The $J_2$ perturbation will cause all six orbit elements, and thus all six orbit element differences used to describe the relative orbit, to vary with time. This perturbed motion of the orbit elements is separated into short-period, long-period and secular motion.[17] The short and long period motion is cyclic and does not cause unbounded relative orbit grow. The instantaneous motion of a satellite is referred to as the osculating motion. The mean motion is what remains after the short period and long period motions have been removed. This mean motion can be thought of as an orbit averaged motion. The Brouwer-Lyddane theory is used to obtain a first order analytic mapping between the osculating and mean orbit elements at any instance of time.[17,18] Using this theory, given any instantaneous osculating orbit elements, it is possible to compute the corresponding mean orbit elements without performing any averaging computation over time. This is attractive for spacecraft formation flying, where often it is not necessary to control the short or long term period motions of the relative orbit, but rather the focus is to avoid and counter the long-term drift caused by the secular motion.

Although all six orbit elements will vary with time, when mapping the osculating orbit elements to mean orbit elements, only three orbit elements are found to exhibit secular grow due to the $J_2$ gravitational influence. Let the parameter $\epsilon$ be defined as

$$\epsilon(a, e) = 3J_2\left(\frac{r_{eq}}{a(1-e^2)}\right)^2 \tag{20}$$

The mean element differential equations are given by.[19,20]

$$\dot{e}_1(t) = \begin{cases} \dfrac{da}{dt} &= 0 \\ \dfrac{de}{dt} &= 0 \\ \dfrac{di}{dt} &= 0 \end{cases} \tag{21a}$$

$$\dot{\boldsymbol{e}}_2(t) = \begin{cases} \dfrac{\mathrm{d}\Omega}{\mathrm{d}t} &= -\dfrac{\epsilon(a,e)}{2}n\cos i \\[2mm] \dfrac{\mathrm{d}\omega}{\mathrm{d}t} &= \dfrac{\epsilon(a,e)}{4}n\left(5\cos^2 i - 1\right) \\[2mm] \dfrac{\mathrm{d}M_0}{\mathrm{d}t} &= \dfrac{\epsilon(a,e)}{4}n\,\eta\left(3\cos^2 i - 1\right) \end{cases} \tag{21b}$$

Unless noted otherwise, this section assumes that all orbit elements have been mapped into the mean element space. As such, only the secular $J_2$ induced motions are considered. Note the natural split into the orbit elements sets $\boldsymbol{e}_1 = \{a, e, i\}$ and $\boldsymbol{e}_2 = \{\Omega, \omega, M_0\}$ in the mean element differential equations in Eq. (21). Thus, while the mean element set $\boldsymbol{e}_2$ will experience secular drift due to the $J_2$ gravitational perturbation, the rate of drift is constant and solely determined by the invariant mean element set $\boldsymbol{e}_1$.

To predict the *mean* linearized relative motion using the orbit element difference expressions in Eqs. (6), the differential equations $\dot{\boldsymbol{e}}_2$ in Eqs. (21) could be analytically integrated with respect to time to yield the chief and deputy orbit element time histories $\boldsymbol{e}(t)$ and $\boldsymbol{e}_d(t)$ respectively. Note that only the three uncoupled orbit element difference differential equations $\{\delta\dot{\Omega}, \delta\dot{\omega}, \delta\dot{M}_0\}$ need to be integrated, since the mean $\{a, e, i\}$ elements to not vary under the influence of the $J_2$ gravitational attraction. However, to find the *osculating* linearized relative motion, all twelve differential equations for the chief and deputy osculating orbit elements would have to be solved. Let us focus on computing the mean relative motion between satellites. Since $\dot{\boldsymbol{e}}_2$ is constant, the differential equations $\{\delta\dot{\Omega}, \delta\dot{\omega}, \delta\dot{M}_0\}$ are trivially solved to yield $\{\delta\Omega(t), \delta\omega(t), \delta M_0(t)\}$. However, to use this time dependent orbit element differences in the linearized relative motion solution in Eq. (6), it is still necessary to solve Kepler's equation at each time step to map the time state $t$ into an equivalent true anomaly angle $f$.

The following development will illustrate how this can be avoided to yield a complete analytical solution of the linearized relative motion (in mean element space) using the true anomaly angle $f$ as the independent variable. Taking the first variation of $\dot{\boldsymbol{e}}_2$, we are able to estimate how the small orbit element differences $\delta\boldsymbol{e}_1 = \{\delta a, \delta e, \delta i\}$ will affect the orbit element difference rates $\delta\dot{\boldsymbol{e}}_2 = \{\delta\dot{\Omega}, \delta\dot{\omega}, \delta\dot{M}_0\}$.

$$\delta\dot{\Omega}(t) = \epsilon\, n\left(\frac{7}{4}\cos i\,\frac{\delta a}{a} - 2\frac{e}{\eta^2}\cos i\,\delta e + \frac{1}{2}\sin i\,\delta i\right) \tag{22a}$$

$$\delta\dot{\omega}(t) = \epsilon\, n\left(-\frac{7}{8}(5\cos^2 i - 1)\frac{\delta a}{a} + \frac{e}{\eta^2}(5\cos^2 i - 1)\delta e - \frac{5}{4}\sin(2i)\,\delta i\right) \tag{22b}$$

$$\delta\dot{M}_0(t) = \epsilon\, n\left(-\frac{7}{8}\eta(3\cos^2 i - 1)\frac{\delta a}{a} + \frac{3}{4}\frac{e}{\eta}(3\cos^2 i - 1)\delta e - \frac{3}{4}\eta\sin(2i)\,\delta i\right) \tag{22c}$$

Next, these differential equations are multiplied by $\mathrm{d}t/\mathrm{d}f$ in Eq. (13) to obtain $\delta\boldsymbol{e}_2'$.

$$\delta\Omega'(f) = \epsilon\underbrace{\left(\frac{7}{4}\cos i\,\frac{\delta a}{a} - 2\frac{e}{\eta^2}\cos i\,\delta e + \frac{1}{2}\sin i\,\delta i\right)}_{\delta\kappa_\Omega}\frac{\eta^3}{(1 + e\cos f)^2} \tag{23a}$$

$$\delta\omega'(f) = \epsilon\underbrace{\left(-\frac{7}{8}(5\cos^2 i - 1)\frac{\delta a}{a} + \frac{e}{\eta^2}(5\cos^2 i - 1)\delta e - \frac{5}{4}\sin(2i)\,\delta i\right)}_{\delta\kappa_\omega}\frac{\eta^3}{(1 + e\cos f)^2} \tag{23b}$$

$$\delta M_0'(f) = \epsilon \underbrace{\left( -\frac{7}{8}\eta(3\cos^2 i - 1)\frac{\delta a}{a} + \frac{3}{4}\frac{e}{\eta}(3\cos^2 i - 1)\delta e - \frac{3}{4}\eta\sin(2i)\,\delta i \right)}_{\delta\kappa_M} \frac{\eta^3}{(1 + e\cos f)^2}$$

(23c)

Note that the terms $\delta\kappa_\Omega$, $\delta\kappa_\omega$ and $\delta\kappa_M$ are constants since the mean $\delta a$, $\delta e$ and $\delta i$ orbit element differences to not vary under the influence of the $J_2$ gravitational perturbation. Making use of the integral expression in Eq. (15), these differential equations are integrated with respect to the true anomaly angle $f$ to yield:

$$\delta\Omega(f) = \delta\Omega(f_0) + \epsilon\,\delta\kappa_\Omega \left( E(f) - \frac{e\,\eta\sin f}{(1 + e\cos f)} \right)\bigg|_{f_0}^{f}$$

(24a)

$$\delta\omega(f) = \delta\omega(f_0) + \epsilon\,\delta\kappa_\omega \left( E(f) - \frac{e\,\eta\sin f}{(1 + e\cos f)} \right)\bigg|_{f_0}^{f}$$

(24b)

$$\delta M_0(f) = \delta M_0(f_0) + \epsilon\,\delta\kappa_M \left( E(f) - \frac{e\,\eta\sin f}{(1 + e\cos f)} \right)\bigg|_{f_0}^{f}$$

(24c)

The current mean anomaly difference $\delta M(f)$ is found by substituting the $\delta M_0(f)$ into Eq. (16). With these analytic solutions to the mean $\delta\Omega(f)$, $\delta\omega(f)$ and $\delta M(f)$ behavior, using Eq. (6) we have an analytic solution to the mean linearized relative orbit motion with the $J_2$ gravitational perturbation included. If we assume that the chief orbit is only weakly linear, then we can approximate the term

$$\left( E(f) - \frac{e\,\eta\sin f}{(1 + e\cos f)} \right)\bigg|_{f_0}^{f} \approx (f - 2e\sin f)\bigg|_{f_0}^{f}$$

(25)

in Eq. (24). The terms $\delta\kappa_\Omega$, $\delta\kappa_\omega$ and $\delta\kappa_M$ reduce to

$$\delta\kappa_\Omega = \frac{7}{4}\cos i\frac{\delta a}{a} - 2e\cos i\,\delta e + \frac{1}{2}\sin i\,\delta i$$

(26)

$$\delta\kappa_\omega = -\frac{7}{8}(5\cos^2 i - 1)\frac{\delta a}{a} + e(5\cos^2 i - 1)\delta e - \frac{5}{4}\sin(2i)\,\delta i$$

(27)

$$\delta\kappa_M = -\frac{7}{8}\eta(3\cos^2 i - 1)\frac{\delta a}{a} + \frac{3}{4}e(3\cos^2 i - 1)\delta e - \frac{3}{4}\eta\sin(2i)\,\delta i$$

(28)

If the chief orbit is near circular, then all terms containing $e$ are dropped leading to the simplified term:

$$\left( E(f) - \frac{e\,\eta\sin f}{(1 + e\cos f)} \right)\bigg|_{f_0}^{f} \approx (f - f_0)$$

(29)

and the expressions:

$$\delta\kappa_\Omega = \frac{7}{4}\cos i\frac{\delta a}{a} + \frac{1}{2}\sin i\,\delta i$$

(30)

$$\delta\kappa_\omega = -\frac{7}{8}(5\cos^2 i - 1)\frac{\delta a}{a} - \frac{5}{4}\sin(2i)\,\delta i$$

(31)

$$\delta\kappa_M = -\frac{7}{8}\eta(3\cos^2 i - 1)\frac{\delta a}{a} - \frac{3}{4}\eta\sin(2i)\,\delta i$$

(32)

Note that this elegant analytical solution to the orbit element differences $\delta e(f)$ is only possible since for the mean motion the $\delta \dot{e}_2(t)$ rates only depend on the constant mean $e_1$ and $\delta e_1$ parameters. When computing the $\delta e_2'(f)$ rates the expressions do depend on the independent variable $f$, but are still analytically integrable. In comparison, to find the osculating linearized relative motion, it is necessary to numerical integrate the 12 orbit element differential equations $e'(f)$ and $e_d'(f)$ for the chief and deputy satellites to obtain the required $\delta e(f)$ values.

## DRIFT DUE TO ATMOSPHERIC DRAG

In LEO the rare atmospheric drag can still have a noticeable effect on the spacecraft orbits. The dominant effects are a circularizing behavior of the orbit geometry and a loss of orbit energy (semi-major axis becomes smaller). Let $\rho$ be the local atmospheric density, $C_d$ the coefficient of drag, $A$ be the projected cross-sectional area, and $m$ be the spacecraft mass. Let the coefficient $B$ be defined through

$$B = \left(\frac{A}{m}\right) C_d \tag{33}$$

Using a form of Gauss' variational equations, the atmospheric drag effect on the orbital elements can be written as[19, 20]

$$\frac{\mathrm{d}a}{\mathrm{d}t} = -B\,\rho\frac{v^3}{an^2} \tag{34a}$$

$$\frac{\mathrm{d}e}{\mathrm{d}t} = -B\,\rho(e + \cos f)v \tag{34b}$$

$$\frac{\mathrm{d}i}{\mathrm{d}t} = 0 \tag{34c}$$

$$\frac{\mathrm{d}\Omega}{\mathrm{d}t} = 0 \tag{34d}$$

$$\frac{\mathrm{d}\omega}{\mathrm{d}t} = -B\,\rho\frac{\sin f}{e}v \tag{34e}$$

$$\frac{\mathrm{d}M_0}{\mathrm{d}t} = \frac{b}{ae}B\,\rho\left(1 + e^2\frac{r}{p}\right)\sin f\,v \tag{34f}$$

where the current velocity magnitude $v$ is written in terms of the true anomaly angle $f$ as

$$v = \frac{h}{p}\sqrt{1 + 2e\cos f + e^2} \tag{35}$$

and the density $\rho(f)$ will be altitude dependent. Note that neither the inclination angle $i$ nor the ascending node $\Omega$ are influenced by this atmospheric drag model.

As written, numerically solving these heavily coupled differential equations requires solving Kepler's equation at each time step. By multiplying the differential equation $\dot{e} = \mathrm{d}e/\mathrm{d}t$ in Eq. (34) by $\mathrm{d}t/\mathrm{d}f$, given in Eq. (35), we are able to rewrite the orbit element differential equations with respect to $f$ as $e' = \mathrm{d}e/\mathrm{d}f$. Numerically solving $e'$ and using the true anomaly as the independent variable avoids having to solve Kepler's equation at each time step. To determine the required $\delta e(f)$ states, the 12 differential equations for the chief

and deputy satellite are first numerically integrated and then differenced. Note that by numerically solving each satellite orbit element differential equations, it is possible for each satellite to have different cross-sectional areas $A$, mass $m$, or coefficient of drag $C_d$.

Next, let us develop first order differential equations $\delta\dot{\boldsymbol{e}}(t)$ which directly approximate how the orbit element differences $\delta\boldsymbol{e}(t)$ will evolve. Taking the first variation of Eq. (34a), small variations in the semi-major axis $\delta a$ will evolve through

$$\delta\dot{a} = \frac{\partial\dot{a}}{\partial a}\delta a + \frac{\partial\dot{a}}{\partial e}\delta e + \frac{\partial\dot{a}}{\partial f}\delta f + \frac{\partial\dot{a}}{\partial B}\delta B \tag{36}$$

where the term $\delta B$ captures differences in the satellites coefficients of drag $C_{d_i}$, cross-sectional areas $A_i$, and masses $m_i$. Since the relative orbit is described in terms of a mean anomaly difference $\delta M$ and not a true anomaly difference $\delta f$, Kepler's equations is used to find a relationship between $\delta f$ in terms of $\delta M$ and $\delta e$.

$$\delta f = \frac{(1 + e\cos f)^2}{\eta^3}\delta M + \frac{\sin f}{\eta^2}(2 + e\cos f)\delta e \tag{37}$$

The procedure outlined in Eqs. (36) and (37) is repeated for the remaining non-zero drag induced orbit element drift equations. Their final form is written as

$$\begin{pmatrix} \delta\dot{a} \\ \delta\dot{e} \\ \delta\dot{\omega} \\ \delta\dot{M}_0 \end{pmatrix} = \underbrace{\begin{bmatrix} K_{a/a} & K_{a/e} & K_{a/M} & K_{a/B} \\ K_{e/a} & K_{e/e} & K_{e/M} & K_{e/B} \\ K_{\omega/a} & K_{\omega/e} & K_{\omega/M} & K_{\omega/B} \\ K_{M/a} & K_{M/e} & K_{M/M} & K_{M/B} \end{bmatrix}}_{[K]} \begin{pmatrix} \delta a \\ \delta e \\ \delta M_0 \\ \delta B \end{pmatrix} \tag{38}$$

with the $[K]$ matrix element defined as

$$K_{a/a} = -\frac{B\rho a}{2\mu}v^3 \tag{39a}$$

$$K_{a/e} = -3B\rho\frac{a^3}{r^2}\cos f\, v \tag{39b}$$

$$K_{a/M} = 3B\rho\frac{a^3}{r^2}\frac{e}{\eta}\sin f\, v \tag{39c}$$

$$K_{a/B} = -\frac{\rho}{a\eta^2}v^3 \tag{39d}$$

$$K_{e/a} = \frac{B\rho}{2a}(e + \cos f)v \tag{39e}$$

$$K_{e/e} = -\frac{B\rho\mu}{8a\eta^4 v}\Big(4 + e^2 - 8e^4 + e(26 - 12e^2)\cos f$$
$$+ (12 + 20e^2)\cos(2f) + (14e + 4e^3)\cos(3f) + 3e^2\cos(4f)\Big) \tag{39f}$$

$$K_{e/M} = \frac{B\rho\mu a}{\eta v r^2}(1 + 2e^2 + 3e\cos f)\sin f \tag{39g}$$

$$K_{e/B} = -\rho(e + \cos f)v \tag{39h}$$

$$K_{\omega/a} = \frac{B\rho}{2ae}\sin f v \tag{39i}$$

13

$$K_{\omega/e} = -\frac{B\rho\mu\sin f}{4ae^2\eta^4 v}\Big(-4 + 14e^2 + 6e^4 + e(4 + 25e^2)\cos f$$
$$+ 2e^2(7 + e^2)\cos(2f) + 3e^3\cos(3f)\Big) \tag{39j}$$

$$K_{\omega/M} = -\frac{B\rho\mu a}{2er^2 v}\big(e + 2(1 + e^2)\cos f + 3e\cos(2f)\big) \tag{39k}$$

$$K_{\omega/B} = -\rho\frac{\sin f}{e}v \tag{39l}$$

$$K_{M/a} = -\frac{B\rho vr}{2a^2 e\eta}\big(1 + e^2 + e\cos f\big)\sin f \tag{39m}$$

$$K_{M/e} = \frac{B\rho\mu\sin f}{4ae^2\eta^3 v}\Big(-4 + 14e^2 + 8e^4 + e(4 + 29e^2)\cos f$$
$$+ 2e^2(7 + 2e^2)\cos(2f) + 3e^3\cos(3f)\Big) \tag{39n}$$

$$K_{M/M} = \frac{B\rho\mu}{8ae\eta^4 v}\Big(e(12 + 25e^2 + 8e^4) + 2(4 + 21e^2 + 14e^4)\cos f$$
$$+ 4e(5 + 7e^2)\cos(2f) + 2e^2(7 + 2e^2)\cos(3f) + 3e^3\cos(4f)\Big) \tag{39o}$$

Note that the $[K]$ matrix elements depend on the chief orbit elements $\dot{e}$. This means that the $\delta\dot{e}$ and the $\dot{e}$ differential equations must be solved simultaneously for the most general case. Multiplying Eq. (39) by the $\mathrm{d}t/\mathrm{d}f$ expression in Eq. (13) allows us to numerically solve $\delta e'$ and avoid solving Kepler's equation at each time step. However, note that no compact analytical solution of $\delta e'(f)$ has been found for this atmospheric drag case. When studying the gravitational $J_2$ perturbation, it was possible to write the secular drift in terms of mean orbit elements which did not explicitly depend on the true anomaly $f$. With the atmospheric drag differential equations $\delta e'(f)$ the integration parameter $f$ appears in complex functions. Thus, while the difference equations in Eq. (39) can be of analytical interest, to obtain the relative orbit motion using the orbit element difference description of Eq. (6), certain differential equations must be solved. Instead of using the approximate $\delta e'(f)$ differential equations along with the chief orbit $\dot{e}(f)$ differential equations, it is recommended to numerically solve the general differential equations $e'(f) = \dot{e}(t)\frac{\mathrm{d}t}{\mathrm{d}f}$ for both the chief and deputy satellites and to compute the desired orbit elements differences through $\delta e(f) = e_d(f) - e(f)$.

## NUMERICAL EXAMPLES

The following numerical simulations illustrate the relative motion approximation in Eqs. (6) with non-constant orbit element differences. Let the chief orbit be given by the orbit elements shown in Table 1.

The orbit element difference sets which define the relative orbits for either case are given in Table 2. Parameter set 1 is defines the relative orbit for the Keplerian motion case, while parameter set 2 defines the mean element space relative orbit for the $J_2$ perturbation case.

The first simulation assumes Keplerian motion. However, the orbit element difference set 1 contains a non-zero $\delta a$ value which will cause a non-zero mean anomaly drift $\delta M'$. The second simulation shows how the orbit element differences will evolve in mean element space under the influence of the $J_2$ gravitational perturbation. For the relative orbits studied, the

**Table 1: Chief Orbit Elements**

| Orbit Elements | Value | Units |
|:---:|:---:|:---|
| $a$ | 7555 | km |
| $e$ | 0.13 | |
| $i$ | 48.0 | deg |
| $\Omega$ | 20.0 | deg |
| $\omega$ | 10.0 | deg |
| $M_0$ | 0.0 | deg |

**Table 2: Orbit Element Differences Defining the Spacecraft Formation Geometry**

| Orbit Elements | Value Set 1 | Value Set 2 | Units |
|:---:|:---:|:---:|:---|
| $\delta a$ | 0.1 | 0.01 | km |
| $\delta e$ | 0.00095316 | 0.001 | |
| $\delta i$ | 0.0060 | -0.010 | deg |
| $\delta \Omega$ | 0.100 | 0.100 | deg |
| $\delta \omega$ | 0.100 | 0.100 | deg |
| $\delta M_0$ | -0.100 | -0.100 | deg |

ratio $\rho/r$ is about 0.003. The chief orbit eccentricity of 0.13 is noticeably larger than this. The results of both the general orbit element drift predictions and the small-eccentricity orbit element drift predictions are compared to the true nonlinear orbit element difference evolution.

Figure 2 compares the mean anomaly drift approximations of Eq. (16) (solid line) and Eq. (18) (dashed line) to the true nonlinear solution. On the scale shown, both mean anomaly difference predictions are virtually identical. Figure 2(b) presents the drift approximations errors on a logarithmic scale over 8 orbits. While the small eccentricity approximation does yield noticeably worse predictions, over a few orbits these errors are all still very small in magnitude. The corresponding relative orbit is illustrated in Figure 3(a).

Figure 4 compares the mean element drift approximations for the second case which includes the $J_2$ perturbation. The solid line illustrates the solution for generally eccentric orbits, while the dashed line shows the linear eccentricity solution. The linear eccentricity case does provide worse $\delta e(f)$ predictions, as expected. However, despite the relatively large chief eccentricity $e$, these errors are still rather small over a few orbit periods. The corresponding relative orbit is illustrated in Figure 3(b).

## CONCLUDING REMARKS

Analytical solutions are presented for the linearized relative orbit problem including secular drift for the case of general Keplerian orbits and the case of studying the mean motion under the $J_2$ gravitational perturbation. This development extends the orbit element difference description to include these cases of time-dependent orbit elements and orbit element differences. If no analytical solution is available, such as is the case with the atmospheric
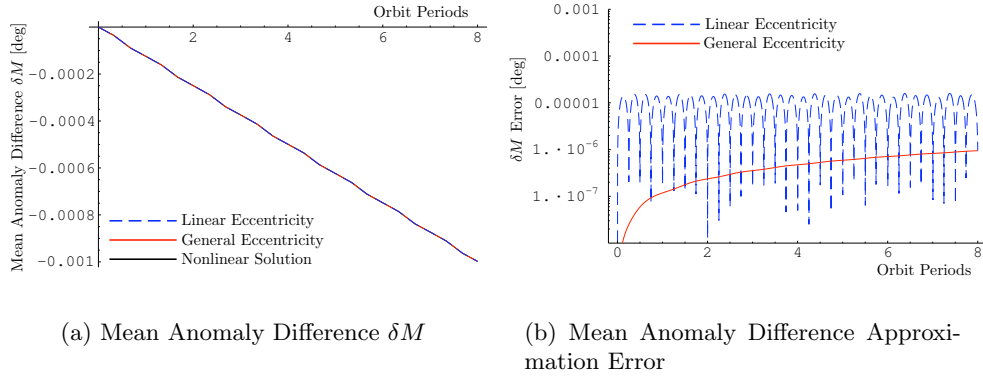
(a) Mean Anomaly Difference $\delta M$

(b) Mean Anomaly Difference Approximation Error

**Figure 2: Orbit Element Difference Drift Predictions for the Parameter Set 1 with Keplerian Orbits.**

drag case, then the chief orbit elements and the relative orbit element differences will need to be numerically integrated. For general perturbations the orbit element difference description studied is still valid, but does not provide an analytical solution to the linearized relative orbit motion.

## REFERENCES

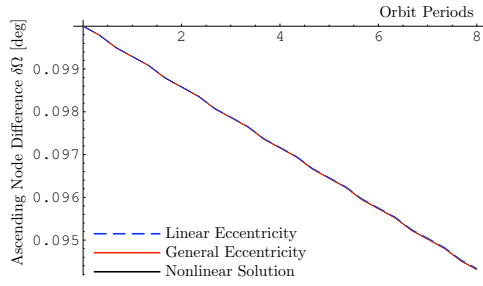[1] PARKER, TIMOTHY W., JACQUES, DAVID R., and WIESEL, WILLIAM E., "Ad-



(a) LVLH Orbit for Parameter Set 1 with Keplerian Orbits

(b) LVLH Orbit for Parameter Set 2 with $J_2$ Perturbation
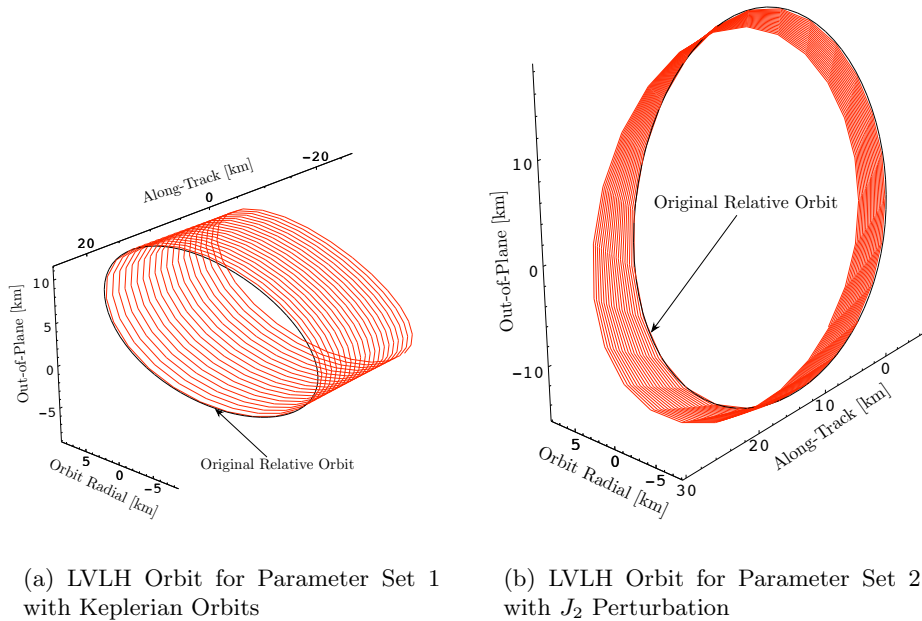
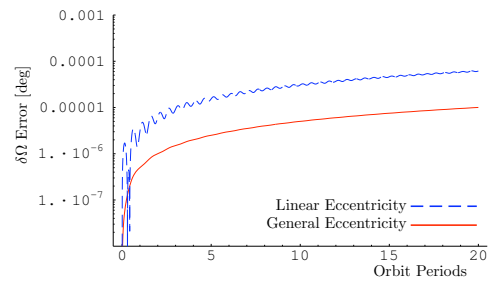**Figure 3: LVLH Illustrations of Relative Orbits.**
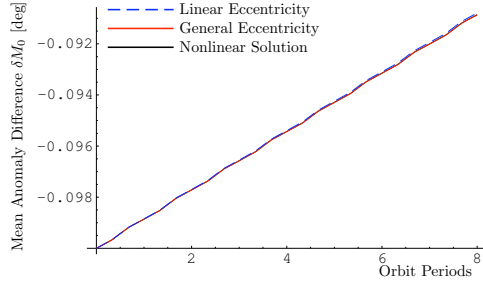
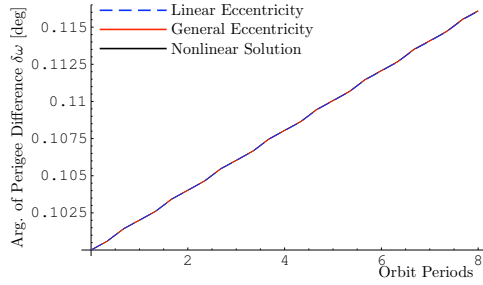(a) Initial Mean Anomaly Difference $\delta M_0$
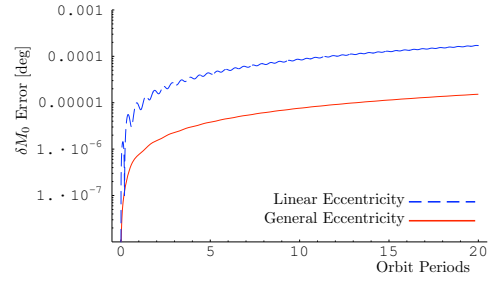
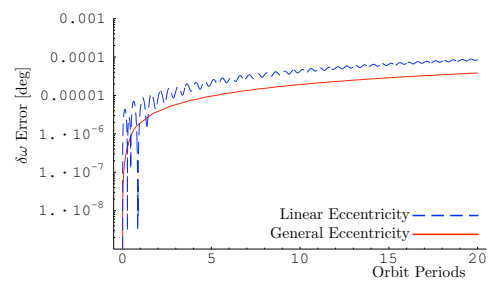(b) Initial Mean Anomaly Difference Approximation Error

(c) Ascending Node Difference $\delta \Omega$

(d) Ascending Node Difference Approximation Error

(e) Argument of Perigee Difference $\delta \omega$

(f) Argument of Perigee Difference Approximation Error

Figure 4: **Mean Orbit Element Difference Drift Predictions for the Parameter Set 2 with $J_2$ Perturbations.**

vanced Metrics for Optimizing Satellite Formations Performing Interferometry Missions", *AIAA/AAS Astrodynamics Specialist Conference and Exhibit*, Monterey, CA, Aug. 5–8 2002, Paper No. AIAA 2002-4740.

[2] MELTON, ROBERT G., "Time-Explicit Representation of Relative Motion Between Elliptical Orbits", *Journal of Guidance, Control, and Dynamics*, Vol. 23, No. 4, 2000, pp. 604–610.

[3] TSCHAUNER, J. and HEMPEL, P., "Rendezvous zu einem in Elliptischer Bahn Umlaufenden Ziel", *Astronautica Acta*, Vol. 11, 1965, pp. 104–109.

[4] CARTER, THOMAS E., "State Transition Matrix for Terminal Rendezvous Studies: Brief Survey and New Example", *Journal of Guidance, Navigation and Control*, Vol. 31, No. 1, 1998, pp. 148–155.

[5] KECHICHIAN, J. and KELLY, T., "Analytical Solution of Perturbed Motion in Near-Circular Orbit Due to J2, J3 Earth Zonal Harmonics in Rotating and Inertial Cartesian Reference Frames", *AIAA 27th Aerospace Sciences Meeting*, Reno, Nevada, January 1989, Paper No. 89-0352.

[6] BROUCKE, ROGER A., "A Solution of the Elliptic Rendezvous Problem with the Time as Independent Variable", *AAS/AIAA Space Flight Mechanics Meeting*, San Antonio, TX, January 2002, Paper No. AAS 02-144.

[7] SCHAUB, HANSPETER and ALFRIEND, KYLE T., "$J_2$ Invariant Reference Orbits for Spacecraft Formations", *Celestial Mechanics and Dynamical Astronomy*, Vol. 79, 2001, pp. 77–95.

[8] ALFRIEND, KYLE T. and SCHAUB, HANSPETER, "Dynamics and Control of Spacecraft Formations: Challenges and Some Solutions", *Journal of the Astronautical Sciences*, Vol. 48, No. 2 and 3, April–Sept. 2000, pp. 249–267.

[9] GARRISON, JAMES L., GARDNER, THOMAS G., and AXELRAD, PENINA, "Relative Motion in Highly Elliptic Orbits", *AAS/AIAA Space Flight Mechanics Meeting*, Albuquerque, NM, Feb. 1995, Paper No. 95-194.

[10] CHICHKA, DAVID F., "Satellite Cluster with Constant Apparent Distribution", *Journal of Guidance, Control and Dynamics*, Vol. 24, No. 1, Jan.–Feb. 2001, pp. 117–122.

[11] HUGHES, STEVEN P. and HALL, CHRISTOPHER D., "Optimal Configurations of Rotating Spacecraft Formations", *Journal of the Astronautical Sciences*, Vol. 48, No. 2 and 3, April–Sept. 2000, pp. 225–247.

[12] JUNKINS, JOHN L., AKELLA, MARUTHI R., and ALFRIEND, KYLE T., "Non-Gaussian Error Propagation in Orbital Mechanics", *Journal of the Astronautical Sciences*, Vol. 44, No. 4, Oct.–Dec. 1996, pp. 541–563.

[13] SCHAUB, HANSPETER and ALFRIEND, KYLE T., "Hybrid Cartesian and Orbit Element Feedback Law for Formation Flying Spacecraft", *Journal of Guidance, Control and Dynamics*, Vol. 25, No. 2, March–April 2002, pp. 387–393.

[14] SCHAUB, HANSPETER, "Spacecraft Relative Orbit Geometry Description Through Orbit Element Differences", *14th U.S. National Congress of Theoretical and Applied Mechanics*, Blacksburg, VA, June 2002.

[15] HILL, GEORGE, "Researches in the Lunar Theory", *American Journal of Mathematics*, Vol. 1, 1878, pp. 5–26.

[16] CLOHESSY, W. H. and WILTSHIRE, R. S., "Terminal Guidance System for Satellite Rendezvous", *Journal of the Aerospace Sciences*, Vol. 27, No. 9, Sept. 1960, pp. 653–658.

[17] BROUWER, DIRK, "Solution of the Problem of Artificial Satellite Theory Without Drag", *The Astronomical Journal*, Vol. 64, No. 1274, 1959, pp. 378–397.

[18] LYDDANE, R. H., "Small Eccentricities or Inclinations in the Brouwer Theory of the Artificial Satellite", *The Astronomical Journal*, Vol. 68, No. 8, October 1963, pp. 555–558.

[19] BATTIN, RICHARD H., *An Introduction to the Mathematics and Methods of Astrodynamics*, AIAA Education Series, New York, 1987.

[20] SCHAUB, HANSPETER and JUNKINS, JOHN L., *Analytical Mechanics of Space Systems*, AIAA Education Series, 2003, currently in press.